

## Article

# Fabrication of Nano-Silver–Silver Ion Composite Antibacterial Agents for Green Powder Coatings

Haiping Zhang <sup>1</sup>, Jixing Cui <sup>1</sup>, Jesse Zhu <sup>1,2</sup> , Yuanyuan Shao <sup>3,4</sup> and Hui Zhang <sup>2,5,\*</sup>

- <sup>1</sup> School of Chemical Engineering and Technology, Tianjin University, Tianjin 300072, China  
<sup>2</sup> Department of Chemical and Biochemical Engineering, Western University, London, ON N6A 3K7, Canada  
<sup>3</sup> Nottingham Ningbo China Beacons of Excellence Research and Innovation Institute, The University of Nottingham Ningbo China, Ningbo 315100, China  
<sup>4</sup> Particle Technology Industrial Engineering Center, Zhejiang Institute of Tianjin University, Shaoxing 312300, China  
<sup>5</sup> School of Chemical Engineering and Light Industry, Guangdong University of Technology, Guangzhou 510006, China  
\* Correspondence: hzhang1@uwo.ca

**Abstract:** Nano-silver is characterized by broad-spectral, strong and stable antibacterial properties, which make it a promising material in coating applications. However, the efficiency of nano-silver is generally low in the coating of films. Here, we developed a series of highly active and durable silver ions–nano-silver antimicrobial agents for powder coatings. To optimize antimicrobial activity and durability, two different nano-silver generation methods, i.e., *in situ* and *ex situ* methods combined with different carrier materials, i.e., zeolite with high ion-exchange ability and montmorillonite of layered structure were adopted and investigated. All four antibacterial additives show high activity with a reduction rate of over 99.99% and R value of over 5. The *ex situ* generated nano-silver antibacterial agents with both carriers exhibit higher activity in the initial antibacterial property and antibacterial durability that the coating films are able to maintain over 99% antimicrobial reduction after 20 cycles (1200 times) of soap solution wiping. They also show a lower yellowish color difference of less than three compared to the films with *in situ* generation method. The one with montmorillonite as carrier shows the stronger antibacterial property with an R value of 5.88 and slightly better film appearance of lower color difference, smaller reduction in gloss and increase in haze as compared to zeolite carrier due to the layered structure.

**Keywords:** antimicrobial agent; powder coating; carrier; nano-silver; *in situ* synthesis; *ex situ* synthesis



**Citation:** Zhang, H.; Cui, J.; Zhu, J.; Shao, Y.; Zhang, H. Fabrication of Nano-Silver–Silver Ion Composite Antibacterial Agents for Green Powder Coatings. *Coatings* **2023**, *13*, 575. <https://doi.org/10.3390/coatings13030575>

Academic Editor: Seunghan Oh

Received: 31 December 2022

Revised: 22 February 2023

Accepted: 2 March 2023

Published: 7 March 2023



**Copyright:** © 2023 by the authors. Licensee MDPI, Basel, Switzerland. This article is an open access article distributed under the terms and conditions of the Creative Commons Attribution (CC BY) license (<https://creativecommons.org/licenses/by/4.0/>).

## 1. Introduction

Powder coating is an environmentally friendly coating, which has the advantages of VOCs free emission, low cost, high efficiency and a high recovery rate of 98% compared with traditional liquid coatings [1,2]. With the increasing improvement in living standards, especially after the outbreak of COVID-19 in 2019, people pay more attention to their health and hygiene conditions. Pathogens can often exist on inanimate surfaces for hours, days, weeks or even longer, e.g., the survival time of COVID-19 on the surface of objects can be up to several days [3,4]. The pollution caused by microorganisms in the home and public environment cannot be ignored. Therefore, functional antibacterial powder coatings, which can kill bacteria and viruses on the surface of objects and cut off the indirect transmission of pathogenic bacteria/viruses, are attracting more and more attention in recent years.

Silver-based antibacterial agents are widely used in coating systems because of their broad-spectrum, stable performance, strong antibacterial property and no resistance to drugs [5]. They not only have good bactericidal effects on Gram-positive bacteria, Gram-negative bacteria and fungi [6], but also have disinfection and sterilization effects on some viruses, such as hepatitis B virus, HIV, etc. [7,8]. The toxicity mechanism is generally

considered as that they can change the cell wall permeability, reduce intracellular energy, destroy the transmembrane proton gradient, occupy enzyme active sites, the denaturation of proteins and generate reactive oxygen species, etc. [9–12].

At present, silver antibacterial agents used in coatings are generally silver ions loaded on zeolite carrier. As a releasing antibacterial agent, silver ions are released through ion exchange with environmental ions and diffuse and migrate to the coating surface to play the bactericidal role. However, antibacterial agents based on ion exchange characteristics are easy to release silver ions under wet conditions or during coating cleaning, resulting in a rapid loss of silver ions and, thus, the poor durability of the coatings [13]. In recent years, nano-silver particle antibacterial agents are expected to solve the problems of excess release and insufficient storage. As another form of silver antibacterial agent, the biological activity of silver nanoparticles is generally considered to be realized by the oxidation to active silver ions [14]. The slow but sustainable release of silver ions from nano-silver causes it to have the potential of a silver ion reservoir and improve the durability of the antibacterial coating [15].

In the previous research, our group developed a nano-silver–silver ion composite antibacterial agent. With nano-silver as the supplement to silver ions, it cooperates with ionic silver to greatly extend the durability of the antibacterial coating. However, commercial silver nanoparticles with large particle sizes (50–60 nm) were used and their activity was relatively low. When the majority of ionic silver was consumed, the efficient bactericidal function cannot be achieved by relying merely on the oxidation of nano-silver [16]. It is reported that the activation reaction of nano-silver mainly occurs on the surface of nanoparticles and its reactivity is directly related to the contact-specific surface area [17,18]. Small particles with large specific surface area generally have strong antibacterial activity. Therefore, in order to achieve the long-term synergistic effect of nano-silver and silver ions, self-made nano-silver was applied instead of large-particle-size commercial nano-silver. There are many ways to prepare nano-silver, including physical, chemical and biological methods [17,19–21]. Biogenic synthetic routes are environmentally friendly, but their relatively poor reproducibility limits their application [22]. The traditional chemical synthesis is facile and repeatable, and is thus adopted in this paper. Nano-silver was prepared in two ways through chemical reduction, namely *in situ* generation and *ex situ* generation. For *in situ* synthesis method, silver ions are directly reduced on the carrier, while nano-silver is pre-made and transferred to the carrier, and subsequently in *ex situ* synthesis method.

In addition, carrier material is also an important parameter influencing the function of the active components. The accommodation of silver ions and nanoparticles on zeolite and montmorillonite carriers are illustrated in Figure 1. The former, which has a strong ion exchange capacity, is often used as a carrier for silver ions [23]. However, it is reported that it is not a good carrier of nano-silver and nano-silver can only adhere to the surface of zeolite particles, which is easy to fall off [16]. Montmorillonite is a good nano-silver carrier, which belongs to layered silicate [24]. Although the ion exchange capacity is weaker than that of zeolite, the interlayer domain can accommodate nano-silver, so the content of nano-silver can be increased by using this carrier. Moreover, due to the limited size of the interlayer domain, the size of silver nanoparticles can be controlled to obtain uniform silver nanoparticles with small particle size. Therefore, this paper also investigated the influence of zeolite carrier suitable to hold silver ions and montmorillonite carrier suitable to accommodate nano-silver. The antibacterial property and durability of the coating were studied on different combinations of the carriers and nano-silver synthesized from different methods. This paper studies a combination effect of the carrier and active component and will provide guidance for the preparation of active and durable nano-silver antibacterial agents, especially to the carrier design and corresponding silver load mode screening.

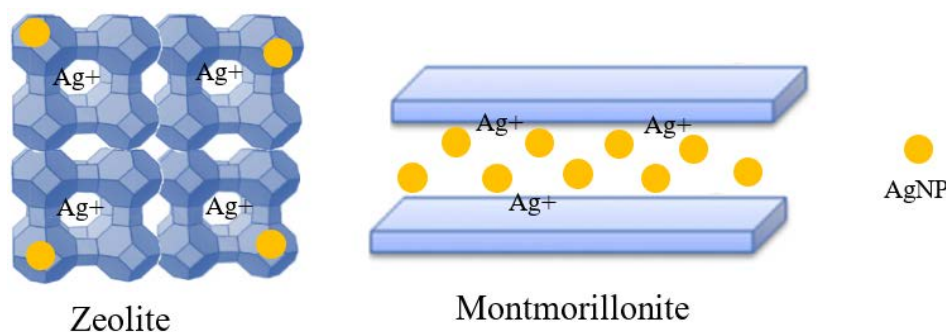


**Figure 1.** Accommodation of silver ions and nanoparticles on zeolite and montmorillonite.

## 2. Experimental Section

### 2.1. Materials

Polyester powder coatings were provided by Guangdong Huajiang Powder Technology Co., Ltd., Zhaoqing, China. Linde type A zeolite and montmorillonite (model K10) were used as carrier materials, which were supplied by PQ Corporation and Clariant Chemicals, respectively. Their SEM images are shown in Figure 2. Silver nitrate ( $\text{AgNO}_3$ , purity > 99.9%), copper nitrate trihydrate ( $(\text{Cu}(\text{NO}_3)_2 \cdot 3\text{H}_2\text{O}$ , purity > 99.9%), zinc nitrate hexahydrate ( $(\text{Zn}(\text{NO}_3)_2 \cdot 6\text{H}_2\text{O}$ , purity > 99.9%),  $\alpha$ -Lipoic acid (LA), sodium methylcellulose (Na-CMC) and sodium alginate (Na-alginate) were purchased from Aladdin Co., Ltd., Tokyo, Japan. Polyacrylamide (PAM) was obtained from Tianjin Yuanli Chemicals. Polyvinylpyrrolidone (PVP), sodium citrate (SC) and sodium borohydride ( $\text{NaBH}_4$ ) were from J&K Scientific Co., Ltd., Beijing, China. *E. coli*, ATCC25922 was obtained from Luwei Technology Co., Ltd., Guangdong, China. Coating substrates used are aluminum plates from Guangzhou Shenghua BEVS Co., Ltd., (Guangzhou, China).

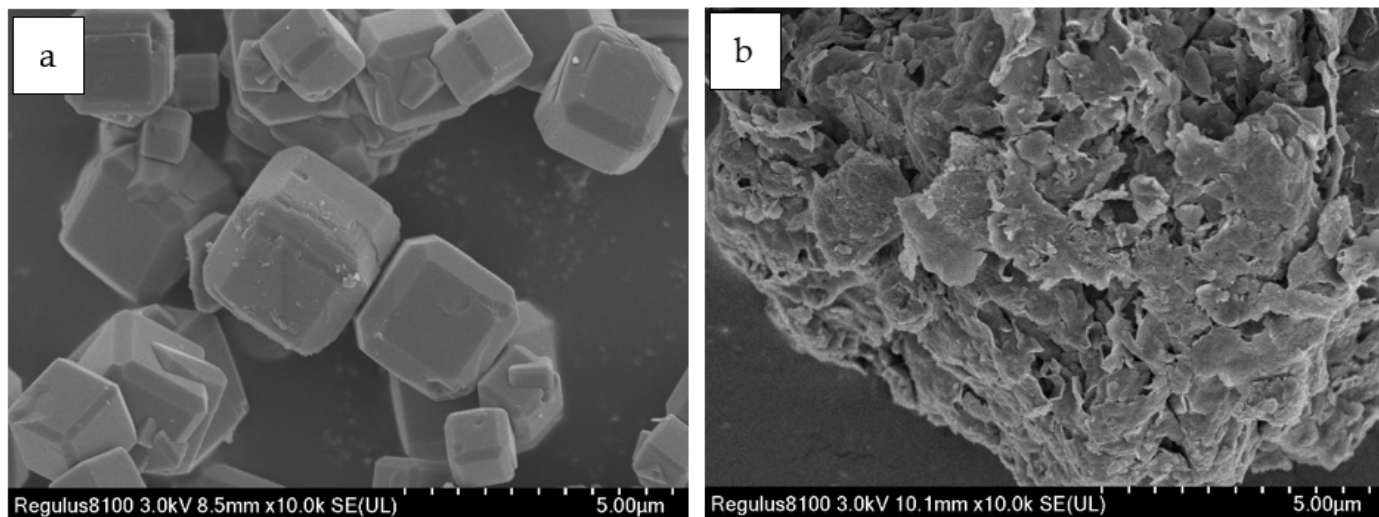


**Figure 2.** SEM images of Linde type A zeolite (a) and montmorillonite (b).

### 2.2. Preparation Process of Antimicrobial Additives and Coatings

#### 2.2.1. Preparation of Additives with In Situ Synthesized Silver Nanoparticles

The carrier material LTA zeolite or montmorillonite was added to 1 mmol/L of  $\text{AgNO}_3$  solution for ion exchange, centrifuged and washed with deionized water. The supernatant was taken and added to 0.1 M NaCl solution during washing to test the presence of ionic silver through the precipitation reaction. After no precipitate,  $\text{AgCl}$  was observed, the solid sample was suspended in 100 mL of deionized water. An amount of 2 mmol/L of  $\text{NaBH}_4$  solution was slowly added into the suspension under continuous stirring. The obtained nano-silver-containing zeolite or montmorillonite was mixed with the solution of

0.03 mol/L silver, 0.06 mol/L copper and 0.06 mol/L zinc ions, stirring for 5 h, then washed and dried following the procedures described in [13]. The solid product was then added to the hydrophilic polymer solution of PAM (1 wt.%), Na-alginate (3 wt.%) and Na-CMC (7 wt.%). After stirring at 60 °C until a viscous liquid was formed, they were transferred to a fume hood for complete dry. The obtained solid was ground into fine powder and screened through 600-mesh sieve. The glassware used was all soaked in 10% nitric acid solution for 2 h and then sterilized with high-pressure steam for 20 min before use.

### 2.2.2. Preparation of Additives with Ex situ Synthesized Silver Nanoparticles

The silver nanoparticles were prepared following the procedures below: 300 mL of 2 mmol/NaBH<sub>4</sub> solution was mixed with 0.3 g of PVP and LA, respectively. Then, different amounts of AgNO<sub>3</sub> solution were slowly added to the solution under constant stirring, and nano-silver was formed. Another group of nano-silver suspension was prepared using 300 mL 2 mmol/L of sodium citrate solution and 50 mL of silver nitrate solution with the similar procedure.

Ion-exchanged LTA zeolite and montmorillonite were prepared according to our previous work [13]. A total of 0.5 g ion-exchanged LTA zeolite or montmorillonite was mixed with the nano-silver suspension and the mixture was stirred for 1 h at room temperature. Then, 1 wt.% of lipoic acid ethanol solution was added and stirring was maintained for another hour. The suspension was then mixed with hydrophilic polymer solution of PAM, Na-alginate and Na-CMC, dried and ground, following the same procedure as the preparation of additives with in situ silver nanoparticles. The additive samples were defined, as shown in Table 1.

**Table 1.** Description and statement of prepared antimicrobial additives.

Sample Name	Synthesis Method of Nano-Silver	Carrier Materials
AgNPs(a)-Z	Ex situ synthesis	Zeolite
AgNPs(a)-M	Ex situ synthesis	Montmorillonite
AgNPs(b)-Z	In situ synthesis	Zeolite
AgNPs(b)-M	In situ synthesis	Montmorillonite

### 2.2.3. Preparation of Antimicrobial Coatings

Polyester powder coating was mixed with antimicrobial additives (2.0 wt.%) and tightly bonded with additive particles using pressure bonding method. The antibacterial powder was sprayed onto the aluminum plate using a corona electrostatic spray gun (Surecoat, Nordson Corp., Westlake, OH, USA) with an operating voltage of 40 kV, air pressure of 5 bar and spaying distance of 40 cm. After spraying, the plate was put into the convection oven (Wanrui Corp., Shanghai, China) for curing. All the samples were cured at 200 °C for 10 min.

## 2.3. Characterization of Antimicrobial Additives and Coatings

### 2.3.1. Characterization of Silver Nanoparticles and Additives

Ultraviolet visible spectrophotometer (DR6000, 190–1100 nm, HACH, Ames, IA, USA) was used to analyze the particle size of nano-silver in the antibacterial agent. The measuring wavelength range was 300–700 nm. A 1 cm quartz cuvette was used to avoid the absorption of ultraviolet light by ordinary glass. Due to the surface plasma effect, nano-silver absorbs light of a specific wavelength and changes with the change of particle size.

The antimicrobial activity of additives was evaluated by the disc diffusion method. An amount of 0.5 mL *E. coli* suspension of approximate cell density of 10<sup>6</sup> colony-forming unit (CFU/m) was added and spread evenly on the Mueller Hinton agar (MH) medium. Small filter paper discs (diameter 6 mm) were first dipped in 1 g/L antibacterial solution and then dried in a dark place. Then, the paper discs containing antibacterial agent were put onto the MH medium and incubated in a biochemical incubator (SPX-70BIII, Tianjin

Taisite Instrument Co., Ltd., Tianjin, China) at 37 °C for 24 h. The diameter of inhibition rings was measured with a vernier caliper. The antimicrobial tests were conducted in the UV sterilization cabinet (UVC-11, Lab Companion, Billerica, MA, USA). All the tests were conducted in triplicate and the average was calculated.

### 2.3.2. Characterization of Antimicrobial Coatings

The antimicrobial activity of the coating was tested according to ASTM E2180-07 standard. Bacterial solutions (approx.  $10^6$  CFU/mL) were taken and dropped onto each test sample and cultured at 37 °C. Samples were taken out from the incubator at different inoculation times and the CFU of microorganisms of each sample was measured. A coating sample without antimicrobial additive was defined as control sample. Each test was performed in triplicate. The reduction rate was calculated as follows:

$$\text{Reduction rate}(\%) = \frac{X_0 - \bar{X}}{X_0} \times 100\% \quad (1)$$

where  $X_0$  stands for the number of organisms after the 6 h incubation period for the control coating and  $\bar{X}$  represents the mean value for that of sample coatings.

To more accurately evaluate the antimicrobial activity, R value [25] of the change in the number of microorganisms was determined in the experiment according to Equation (2).

$$R = \left[ \log\left(\frac{B}{A}\right) - \log\left(\frac{C}{A}\right) \right] = \left[ \log\left(\frac{B}{C}\right) \right] \quad (2)$$

where A represents the number of microorganisms at the initial time, and B and C stand for the average number of microorganisms in the control group and in the antibacterial plate after 6 h, respectively. According to the standard, the judgment standard for the antibacterial ability of the antibacterial board is that the R value is not less than 2, that is, the antibacterial rate is not less than 99%.

The durability activity was tested by wiping method. A sponge (2 cm × 2 cm) soaked with 2.5 g/L dish soap solution fixed on a multifunctional abrasion tester (860, Xiangmin, China) was used to wipe the coatings. An amount of 800 g of weights was applied to insert a pressure of 20 kPa. One cycle is defined as a 60-time back-and-forth wipe. The antimicrobial activity was measured before and after wiping.

The appearance of coatings was also evaluated. The gloss and distinctness of image (DOI) were tested using Rhopoint IQ equipment. The yellowing color change of coating was measured by a colorimeter (WF32, Shanghai Jiabiao, Shanghai, China).

## 3. Results and Discussion

### 3.1. Synthesis of Silver Nanoparticles

Under the reduction action of NaBH<sub>4</sub>, Ag<sup>+</sup> is rapidly reduced to Ag<sup>0</sup>, and these fine Ag<sup>0</sup> quickly merge into crystal nuclei. This process usually occurs within 200 ms and the solution color is light [17]. Then, these nuclei collide and merge continuously to obtain larger nuclei, and nano-silver is obtained through continuous merging and growth. The addition of surface treatment agents inhibits the further growth of the crystals. One end of these surface agents bonds with the nano-silver, and the other end is charged or has repulsive groups, which makes the nano-silver particles repel each other and maintain a good dispersion. With the extension of time, due to the high surface energy of fine particles, they gradually dissolve during the ripening process and promote the gradual growth of large particles, which is a process called Ostwald ripening. When the color of the solution no longer changes, the nano-silver solution after ripening is obtained.

As shown in Figure 1, the state of the nano-silver solution obtained by PVP and LA is similar. According to the electrification of different surface treatment agents, the surface of nano-silver modified by PVP is electrically neutral, and the surface modified by LA is with carboxyl groups. Since the number of hydroxyl groups on the surface of montmorillonite is

less than that of LTA zeolite, it may not be able to firmly bond to the LA terminal carboxyl group, while the long-chain polymer PVP is more easily bound to the montmorillonite microstructure. Therefore, PVP-capped silver nanoparticles are used for montmorillonite carrier, while LTA zeolite selects LA-capped silver nanoparticles.

For nano-silver reduced by sodium citrate, sodium citrate acts as both a reducing agent and surface-treatment agent. As shown in Figure 1, the liquid color is light when sodium citrate is used for reduction, which indicates that the content of nano-silver generated is low. This is mainly due to the weak reduction ability of sodium citrate, so that a large part of silver ions is not reduced. However, sodium citrate has an obvious effect on the growth of crystal nucleus, so it can cooperate with NaBH<sub>4</sub> to control the particle size of nano-silver [17]. In the first stage of the reduction reaction, silver ions are preferentially reduced to form smaller particles. After the formation of nano-silver clusters, the pH of the solution is changed to alkaline. At this time, under the effect of sodium citrate, silver ions are slowly reduced to elemental silver on the surface of nano-silver, promoting the growth of crystal nuclei.

In addition, in order to load more nano-silver onto the carrier, nano-silver with different concentrations was prepared. Figure 3 shows the images and UV visible spectra of nano-silver of different concentrations. As shown in the figure, the maximum absorption peak of the nano-silver with a smaller concentration of 0.001 and 0.01 mg/mL is about 400 nm, which indicates that the nano-silver has smaller particle size. With the increase in concentration, the collision between silver nanoparticles intensifies, larger silver particles are formed, verified by the darker color of the suspension, which is also observed from other research [17,21]. When it is increased to 1 mg/mL, the color of the suspension becomes gray black. It can be seen in the UV spectra that the maximum absorption peak shifts to the right with the increase in concentration, reaching about 450 nm at 1 mg/mL. Moreover, with the increase in concentration, the width of each absorption peak also increases, indicating that the particle size distribution increases and high concentration of nano-silver leads to wider particle size distribution. Although the high concentration of nano-silver suspension can bring convenience to the preparation of antibacterial agents, the larger particle size and distribution are unfavorable to the antibacterial properties. Uniform particle size distribution is beneficial to the antibacterial activity of nano-silver. The absorption peak distribution of 0.05 mg/L nano-silver solution is narrow, the particle size distribution is relatively small, and the maximum absorption peak is about 405 nm, indicating a small particle size of about 10–20 nm, which guarantees a high loading and also a high antibacterial activity of silver nanoparticles.

### 3.2. Antibacterial Property of Composite Antibacterial Agents

The results of the inhibition ring test of the four antibacterial agents against Escherichia coli are shown in Figure 4. It can be seen from the figure that the control group without antibacterial agent does not show any antibacterial area, while all the antibacterial agents show antibacterial areas, indicating that the antibacterial agent has antibacterial activity.

The diameter of inhibition zone determined by vernier caliper is shown in Table 2. It can be seen that all the agents exhibit similar inhibition zone diameter with slight difference. The antibacterial effect of in situ silver nanoparticles is generally weaker than that of ex situ silver nanoparticles. AgNPs(b)-Z shows the weakest antibacterial ability. During the in situ synthesis of AgNP, silver ions were first exchanged in the pores of the zeolite particles. When they were reduced, many of the generated silver particles occupied the internal space of the zeolite, overflowed the pores and covered the surface of the zeolite particles, seriously affecting the subsequent ion exchange process. Therefore, the amount of silver ions that can be exchanged by the antibacterial agent is small, which cannot form a synergistic antibacterial effect of silver nanoparticles and silver ions, and the instant antibacterial property is relatively poor. AgNPs(b)-M performs slightly better than AgNPs(b)-Z, which is due to the different structures of montmorillonite and zeolite. The in situ formation of silver nanoparticles from montmorillonite mainly occurs in the interlayer domain. Due

to the limitation of the interlayer domain, the size of silver nanoparticles generated is smaller, which enhances the antibacterial effect of silver nanoparticles. In addition, the space of interlayer domain becomes larger after the formation of nano-silver, which can be increased from 1.45 nm to 1.54 nm [13,26]. The increased interlayer domain cannot only accommodate a large amount of nano-silver, but also provide more space and sites for subsequent ion exchange.

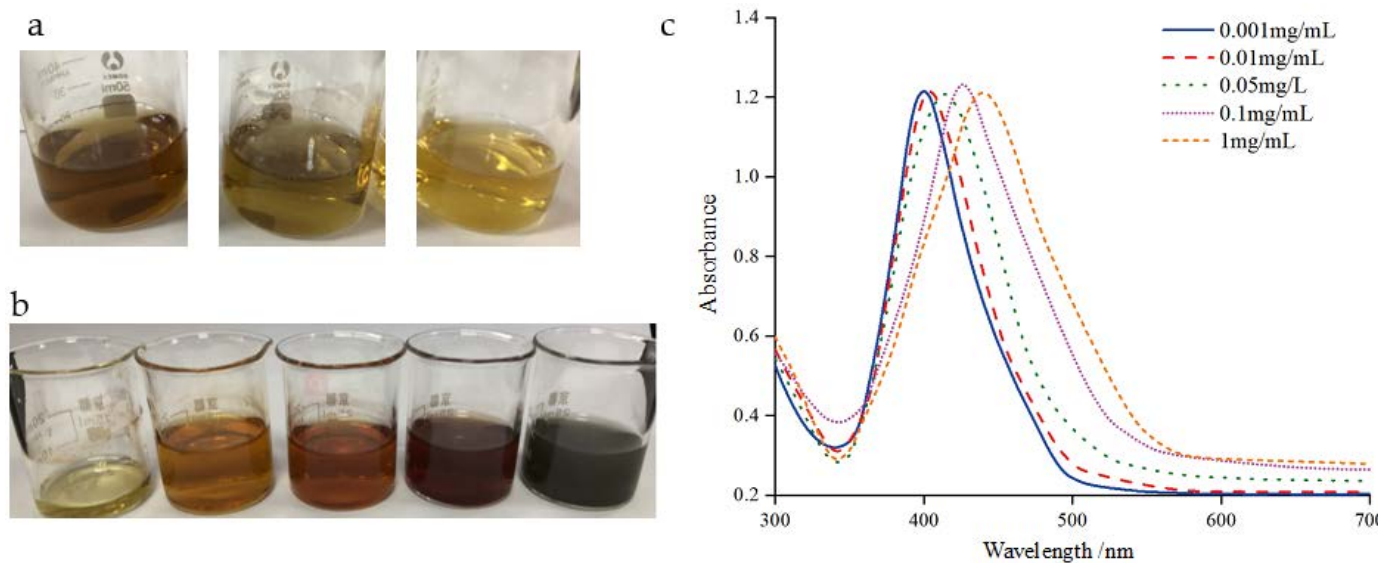


**Figure 3.** (a) Images of AgNPs solutions prepared by different capping agents: PVP, LA and SC (from left to right); (b) images; and (c) UV-vis spectrograms of AgNPs solutions prepared at different concentrations of silver nanoparticles using PVP as capping agent and NaNH<sub>4</sub> and SC as reducing agents: 0.001 mg/mL, 0.01 mg/mL, 0.05 mg/L, 0.1 mg/mL and 1 mg/L (from left to right).

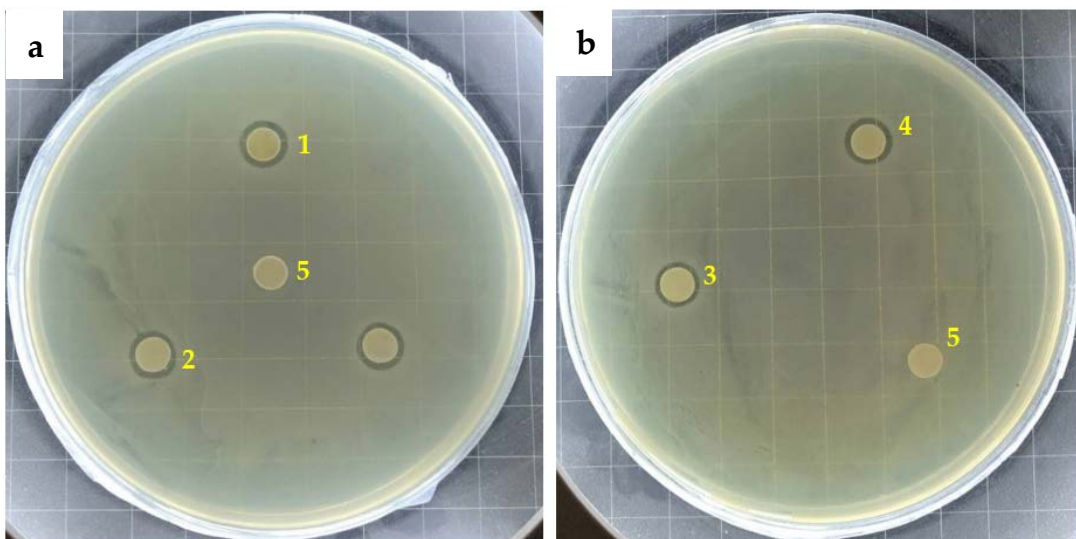


**Figure 4.** Inhibition zone of (a) additives with ex situ synthesized AgNP and (b) additives with in situ synthesized AgNP: 1. AgNPs(a)-Z; 2. AgNPs(a)-M; 3. AgNPs(b)-Z; 4. AgNPs(b)-M; and 5. Control.

**Table 2.** Inhibition zone diameters of the antibacterial agents.

Bacteria Type	Inhibition Zone Diameters (mm)			
	AgNPs(a)-Z	AgNPs(a)-M	AgNPs(b)-Z	AgNPs(b)-M
<i>E. coli</i>	10.40 ± 0.08	9.93 ± 0.05	9.47 ± 0.05	9.73 ± 0.05

Although the silver nanoparticles formed by AgNPs(b)-M in the interlayer domain are smaller in size, usually smaller than 2 nm, the silver nanoparticles are firmly bound in the interlayer domain, which makes oxidation more difficult [27]. Compared with the antibacterial agent AgNPs(a)-M, the added nano-silver is mainly attached to the pores of montmorillonite rather than entering the interlayer domain. The pre-made nano-silver does not occupy the interlayer domain space, which is mainly for the ion exchange sites of silver ions. Therefore, the antibacterial property of AgNPs(a)-M is better than that of AgNPs(b)-M.

Compared with montmorillonite, zeolite carrier is easier to release silver ions. Montmorillonite has more pores and the exchanged ions need to diffuse through the pores, so the instant antibacterial property is slightly poor. In addition, the exchangeable ions, silver, copper and zinc, are in the interlayer domain of montmorillonite and have strong affinity to the carrier, which are difficult to desorb [26]. Therefore, in spite of the small particle size of silver nanoparticles, the instant antibacterial property of AgNPs(a)-M is not as good as AgNPs(a)-Z.

### 3.3. Antibacterial Property and Durability of Antibacterial Coatings

Table 3 shows the antibacterial test results of the antibacterial coatings. The initial number of bacteria is  $3.5 \times 10^6$  CFU/mL; if no antibacterial agent is added, the number of bacteria will increase to  $6.9 \times 10^8$  CFU/mL after 24 h. Compared to the control sample, the number of bacteria on each antibacterial coating film all decreases by 5–6 orders of magnitude, and the reduction rate is more than 99.99%. In order to distinguish the performance of antibacterial coatings, the R value was calculated according to Equation (2). The results show that the R values of the four antibacterial agents are all greater than 5, showing excellent antibacterial properties. The antibacterial property of the antibacterial coatings is slightly different from that of the antibacterial agents, which is due to the different test environment. During the bacteriostatic ring test, which is a closed test environment with insufficient oxygen, nano-silver is difficult to be oxidized. Therefore, the antibacterial activity is mainly from the exchanged silver ions on the carrier. On the other hand, the test environment for coatings is more advantageous, the environmental ions and oxygen are more abundant, and thus, besides the pre-existing silver ions, the antibacterial function of nano-silver is also performed by generating new active ions.

**Table 3.** Antimicrobial performance for the coatings.

Samples	Bacterial No. (0 h) CFU/mL	Bacterial No. (24 h) CFU/mL	Reduction Rate (%)	R Value
Control	$3.5 \times 10^6$	$6.9 \times 10^8$	-	-
AgNPs(a)-Z	$3.5 \times 10^6$	$1.2 \times 10^3$	99.99%	5.76
AgNPs(a)-M	$3.5 \times 10^6$	$9.0 \times 10^2$	99.99%	5.88
AgNPs(b)-Z	$3.5 \times 10^6$	$3.3 \times 10^3$	99.99%	5.26
AgNPs(b)-M	$3.5 \times 10^6$	$3.1 \times 10^3$	99.99%	5.44

The antibacterial agent with montmorillonite as carrier using ex situ generation of silver nanoparticles has more advantages than zeolite. This is because the montmorillonite has a large number of macropores, and the average pore diameter is 6.25 nm, which is much larger than that of LTA zeolite of 0.39 nm. Therefore, there is sufficient space to accommodate pre-made nano-silver, which can be oxidized and ionized to produce silver ions to provide antibacterial activity. In the antibacterial inhibition zone test, the agent with the montmorillonite carrier is weaker than that with zeolite because of the ion internal diffusion. However, the large amount of oxidation ionization from nano-silver makes up for this defect. At the same time, the larger concentration gradient accelerates the diffusion efficiency.

AgNPs(b)-Z and AgNPs(b)-M with in situ nano-silver have weaker antibacterial properties. The reason is consistent with the explanation of the activity of antibacterial

agents. During the preparation process, silver ions were first reduced, and the obtained silver particles occupied the surface of the zeolite or filled the pores of montmorillonite, which hindered the subsequent ion exchange process and therefore decreased immediate antibacterial activity.

Figure 5 and Table S1 show the test results of the durability of antibacterial coatings. The antibacterial activity of the four antibacterial agents after multiple washing and wiping were tested. All the tests were conducted three times and the relative standard deviation was all within 5%, indicating a good repeatability and reliability. Similar to the instant antibacterial property, AgNPs(a)-Z and AgNPs(a)-M produced by the heterotopic reduction of silver nanoparticles also show higher durability, which can withstand over 20 washing cycles (1200 times). The decline of the antibacterial rate of both coatings is relatively gentle, indicating that the release of antibacterial active substances is relatively stable. As analyzed for their instant activity, AgNPs(a)-Z are more inclined to the action of ionic silver, and AgNPs(a)-M is dominated by the synergistic action of ionic silver and nano-silver. Both situations lead to similar durability results. The antimicrobial durability is much better than that of coatings with silver ions, whose antibacterial rate was reduced to lower than 99% after 12 washing cycles [13]. The results verify the reservoir function of silver nanoparticles. Furthermore, AgNPs(a)-M and AgNPs(a)-Z show slightly higher activity when compared with commercial nano-silver agents after 20 washing cycles [16].

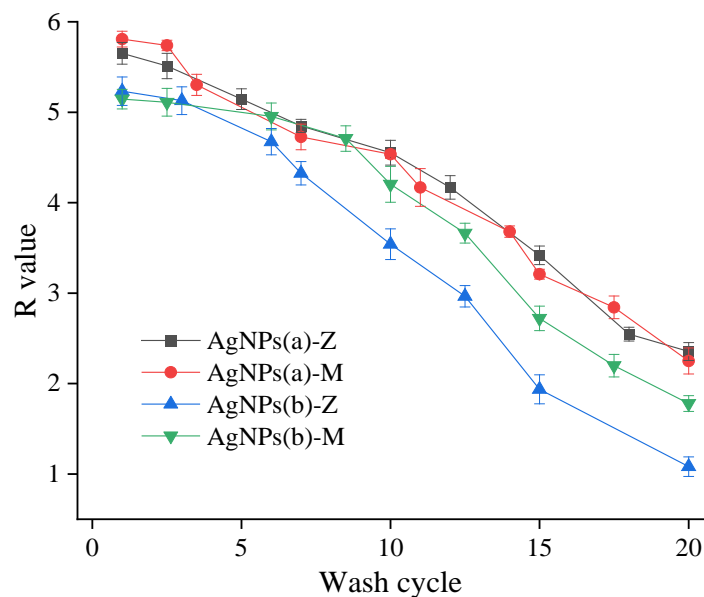


**Figure 5.** Durability of antimicrobial coatings.

The antibacterial agent AgNPs(b)-Z has the lowest antibacterial property, with the reduction rate decreasing to lower than 99% ( $R < 2$ ) at the 15th cycle. Since  $\alpha$ -cage volume of LTA zeolite is very small, about  $700\text{ \AA}^3$ , the obtained silver particles from reduction leave the zeolite interior to the surface under the pressure of the narrow space and adhere to the zeolite surface through van der Waals force, forming a nano-silver layer, which hinders the subsequent silver ion exchange process, resulting in insufficient silver ions of antibacterial agent. During the washing process, silver ions are gradually consumed, and the synergistic effect of nano-silver–silver ions is gradually lost, so the durability is weakened. In addition, the generated nano-silver is weakly bonded with carrier surface by van der Waals force, and the nano-silver is likely to fall off from the zeolite and loses antibacterial ability.

Compared with AgNPs(b)-Z, AgNPs(b)-M with montmorillonite exhibits better durability, since it is a better AgNP carrier that has larger pores where silver nanoparticles can be settled. The nano-silver generated in the early stage mainly exists in the interlayer domain, which is both the storage space of nano-silver and the exchange site of silver ions. With the encapsulation of hydrophilic materials, the synergistic effect of nano-silver–silver

ions is easier to function. However, some literature shows that during the ion exchange process, some silver ions will also replace the nano-silver, extruding the nano-silver out of the interlayer domain and occupying the pores, causing the pores to be blocked and the ion exchange process is thus limited [28,29]. Therefore, its durability is worse than that with ex situ silver nanoparticles.

### 3.4. Appearance of Antibacterial Coatings

The color difference of antibacterial coatings is shown in Figure 6 and Table S2. The yellowing effect is from silver synthesized and silver ions reduced from the curing process. The nano-silver generated in situ has greater yellowing, which is due to the added content of small-particle-size nano-silver generated in situ. In addition, the loaded nano-silver absorbs a large number of silver ions during the subsequent ion exchange process. These silver ions are not formed inside the carrier, but on the surface of the nano-silver, so it is easy to reduce to make the film yellowing during the curing process. It can also be seen that montmorillonite as a carrier has the effect of reducing yellowing. This is because the pores in the montmorillonite are relatively rich, and the complex pores enable nano-silver and silver ions to be included in the montmorillonite, reducing the exposed nano-silver, which has a certain protective effect. At the same time, the diffusion of silver ions to the outer surface requires a certain diffusion energy, so it also partially inhibits the reduction of silver ions. It is worth pointing out that the color changes from the additional nano-silver particles are known, so these changes can be avoided by adjusting the addition of pigments, which may not be an issue in the practical application.

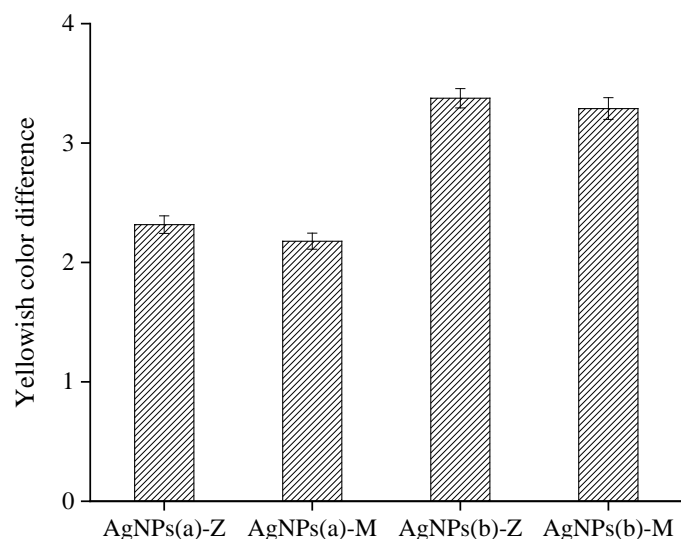


**Figure 6.** Effects of antimicrobial additives on yellowing color difference of the coatings.

Figure 7 and Table S3 show the effect of antibacterial agents on the gloss and haze of the film surface. When there is no antibacterial agent, it shows high gloss and low haze. After adding antibacterial agent, the gloss decreases and haze increases. It can be seen that the haze of the antibacterial coating with montmorillonite as the carrier is low. One reason is that the montmorillonite particles are larger and have less light scattering effect. The other reason is that the nano-silver mainly exists in the pores of the montmorillonite and less when the aggregation of nano-silver is located outside. It was also found that the gloss of the antibacterial coating with ex situ nano-silver decreased to a higher extent, compared to that of the in situ nano-silver. This may be because the in situ nano-silver is closely bound to the carrier and is difficult to be separated from the carrier.

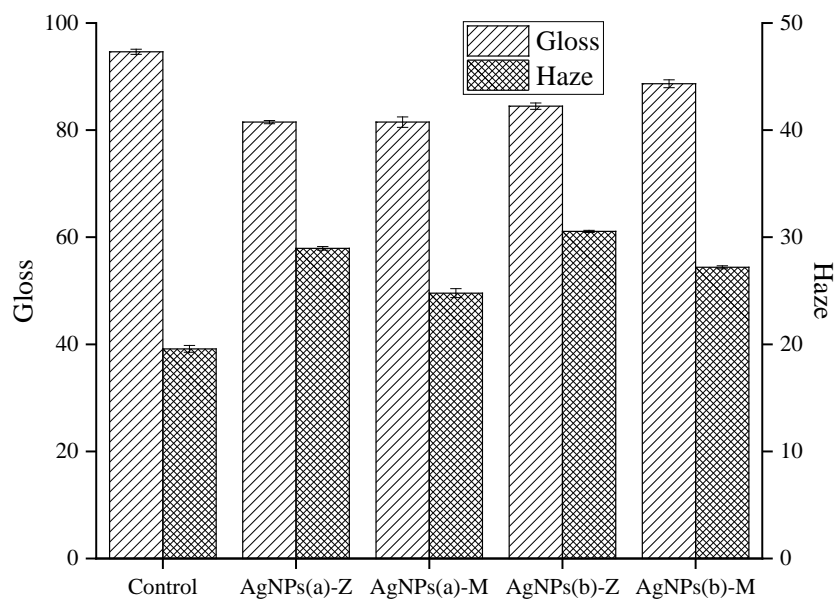


**Figure 7.** Effects of antimicrobial additives on gloss and haze.

#### 4. Conclusions

In this paper, zeolite and montmorillonite were selected as carriers for nano-silver-ionic silver composite antibacterial agents, as zeolite and montmorillonite were good carriers for ionic silver and nano-silver, respectively. Two methods were adopted to prepare silver nanoparticles: ex situ and in situ synthesis methods. In the former method, nano-silver was prepared ex situ and loaded onto the carrier subsequently, while the other is directly generating nano-silver on the carrier. The experimental results show that the ex situ-generated nano-silver antibacterial agent shows better performance on the initial antibacterial property and antibacterial durability, and ex situ-generated nano-silver agent with montmorillonite as carrier has the strongest initial antibacterial property. In terms of coating appearance, the ex situ-generated nano-silver increases the yellowing degree of the coating film to a smaller extent, while the nano-silver with montmorillonite as the carrier has less effect on the film gloss than that with zeolite. It can be concluded that carrier type and loading method of silver nanoparticles play an important role in the antimicrobial activity and coating quality. Therefore, designing a suitable porous carrier with adequate ion-exchangeable sites for accommodating both silver nanoparticles and silver ions is worth exploring, as well as screening the corresponding silver loading methods.

**Supplementary Materials:** The following supporting information can be downloaded at: <https://www.mdpi.com/article/10.3390/coatings13030575/s1>; Table S1: Data sheet for Figure 5; Table S2: Data sheet for Figure 6; Table S3: Data sheet for Figure 7.

**Author Contributions:** Conceptualization, H.Z. (Haiping Zhang), J.Z. and H.Z. (Hui Zhang); methodology, H.Z. (Haiping Zhang), J.C. and Y.S.; validation, Y.S.; investigation, J.C.; writing—original draft preparation, H.Z. (Haiping Zhang) and J.C.; writing—review and editing, H.Z. (Haiping Zhang) and H.Z. (Hui Zhang); supervision, J.Z., Y.S. and H.Z. (Hui Zhang); project administration, J.Z., Y.S. and H.Z. (Hui Zhang); funding acquisition, H.Z. (Haiping Zhang) and H.Z. (Hui Zhang). All authors have read and agreed to the published version of the manuscript.

**Funding:** This work was supported by the Natural Sciences and Engineering Research Council of Canada (Discovery Grant RGPIN-2018-06256) and the National Natural Science Foundation of China (Grant No. 22108198).

**Institutional Review Board Statement:** Not applicable.

**Informed Consent Statement:** Not applicable.

**Data Availability Statement:** The data presented in this study are available in the supplementary material.

**Conflicts of Interest:** The authors declare no conflict of interest.

## References

1. Spyrou, E. *Powder Coatings: Chemistry and Technology*; Vincentz Network GmbH & Co. KG: Hanover, Germany, 2012; pp. 71–77.
2. Huang, J.; Yang, M.; Wan, L.; Tang, K.; Zhang, H.; Chen, J.; Noël, J.J.; Barker, I.; Zhang, H.; Zhu, J. Ultrafine powder coating: Smooth surface, dense structure and enhanced corrosion resistance. *Chem. Eng. J.* **2022**, *455*, 140815. [[CrossRef](#)]
3. Kampf, G.; Todt, D.; Pfaender, S.; Steinmann, E. Persistence of coronaviruses on inanimate surfaces and their inactivation with biocidal agents. *J. Hosp. Infect.* **2020**, *104*, 246–251. [[CrossRef](#)] [[PubMed](#)]
4. van Doremalen, N.; Bushmaker, T.; Morris, D.H.; Holbrook, M.G.; Gamble, A.; Williamson, B.N.; Tamin, A.; Harcourt, J.L.; Thornburg, N.J.; Gerber, S.I.; et al. Aerosol and Surface Stability of SARS-CoV-2 as Compared with SARS-CoV-1. *N. Engl. J. Med.* **2020**, *382*, 1564–1567. [[CrossRef](#)] [[PubMed](#)]
5. Kanwal, Z.; Raza, M.A.; Riaz, S.; Manzoor, S.; Tayyeb, A.; Sajid, I.; Naseem, S. Synthesis and characterization of silver nanoparticle-decorated cobalt nanocomposites (Co@AgNPs) and their density-dependent antibacterial activity. *R. Soc. Open Sci.* **2019**, *6*, 182135. [[CrossRef](#)] [[PubMed](#)]
6. Busila, M.; Musat, V.; Textor, T.; Mahltig, B. Synthesis and characterization of antimicrobial textile finishing based on Ag:ZnO nanoparticles/chitosan biocomposites. *RSC Adv.* **2015**, *5*, 21562–21571. [[CrossRef](#)]
7. Tsai, C.-H.; Whiteley, C.G.; Lee, D.-J. Interactions between HIV-1 protease, silver nanoparticles, and specific peptides. *J. Taiwan Inst. Chem. Eng.* **2019**, *103*, 20–32. [[CrossRef](#)]
8. Kumar, S.D.; Singaravelu, G.; Ajithkumar, S.; Murugan, K.; Nicoletti, M.; Benelli, G. Mangrove-Mediated Green Synthesis of Silver Nanoparticles with High HIV-1 Reverse Transcriptase Inhibitory Potential. *J. Clust. Sci.* **2017**, *28*, 359–367. [[CrossRef](#)]
9. Lok, C.-N.; Ho, C.-M.; Chen, R.; He, Q.-Y.; Yu, W.-Y.; Sun, H.; Tam, P.K.-H.; Chiu, J.-F.; Che, C.-M. Proteomic Analysis of the Mode of Antibacterial Action of Silver Nanoparticles. *J. Proteome Res.* **2006**, *5*, 916–924. [[CrossRef](#)]
10. Khan, A.; Ameen, F.; Khan, F.; Al-Arfaj, A.; Ahmed, B. Fabrication and antibacterial activity of nanoenhanced conjugate of silver (I) oxide with graphene oxide. *Mater. Today Commun.* **2020**, *25*, 101667. [[CrossRef](#)]
11. Bartmanski, M.; Pawlowski, L.; Zielinski, A.; Mielewczik-Gryn, A.; Strugala, G.; Cieslik, B. Electrophoretic Deposition and Characteristics of Chitosan-Nanosilver Composite Coatings on a Nanotubular TiO<sub>2</sub> Layer. *Coatings* **2020**, *10*, 245. [[CrossRef](#)]
12. Azizi-Lalabadi, M.; Garavand, F.; Jafari, S.M. Incorporation of silver nanoparticles into active antimicrobial nanocomposites: Release behavior, analyzing techniques, applications and safety issues. *Adv. Colloid Interface Sci.* **2021**, *293*, 102440. [[CrossRef](#)] [[PubMed](#)]
13. Cui, J.; Yeasmin, R.; Shao, Y.; Zhang, H.; Zhang, H.; Zhu, J. Fabrication of Ag<sup>+</sup>, Cu<sup>2+</sup>, and Zn<sup>2+</sup> Ternary Ion-Exchanged Zeolite as an Antimicrobial Agent in Powder Coating (vol 59, pg 751, 2020). *Ind. Eng. Chem. Res.* **2020**, *59*, 13852. [[CrossRef](#)]
14. Xu, Z.; Zhang, C.; Wang, X.; Liu, D. Release Strategies of Silver Ions from Materials for Bacterial Killing. *ACS Appl. Bio Mater.* **2021**, *4*, 3985–3999. [[CrossRef](#)]
15. Chang, Y.; Cheng, Y.; Feng, Y.; Li, K.; Jian, H.; Zhang, H. Upshift of the d Band Center toward the Fermi Level for Promoting Silver Ion Release, Bacteria Inactivation, and Wound Healing of Alloy Silver Nanoparticles. *Acs Appl. Mater. Interfaces* **2019**, *11*, 12224–12231. [[CrossRef](#)] [[PubMed](#)]
16. Cui, J.; Shao, Y.; Zhang, H.; Zhang, H.; Zhu, J. Development of a novel silver ions-nanosilver complementary composite as antimicrobial additive for powder coating. *Chem. Eng. J.* **2021**, *420*, 127633. [[CrossRef](#)] [[PubMed](#)]
17. Agnihotri, S.; Mukherji, S.; Mukherji, S. Size-controlled silver nanoparticles synthesized over the range 5–100 nm using the same protocol and their antibacterial efficacy. *RSC Adv.* **2014**, *4*, 3974–3983. [[CrossRef](#)]
18. Möhler, J.S.; Sim, W.; Blaskovich, M.A.T.; Cooper, M.A.; Ziora, Z.M. Silver bullets: A new lustre on an old antimicrobial agent. *Biotechnol. Adv.* **2018**, *44*, 1873–1899. [[CrossRef](#)] [[PubMed](#)]
19. Thanh, N.T.K.; Maclean, N.; Mahiddine, S. Mechanisms of Nucleation and Growth of Nanoparticles in Solution. *Chem. Rev.* **2014**, *114*, 7610–7630. [[CrossRef](#)]
20. Baran, A.; Keskin, C.; Baran, M.F.; Huseynova, I.; Khalilov, R.; Eftekhari, A.; Irtegun-Kandemir, S.; Kavak, D.E. Ecofriendly Synthesis of Silver Nanoparticles Using Ananas comosus Fruit Peels: Anticancer and Antimicrobial Activities. *Bioinorg. Chem. Appl.* **2021**, *2021*, 2058149. [[CrossRef](#)]
21. Alissawi, N.; Zaporjchenko, V.; Strunskus, T.; Hrkac, T.; Kocabas, I.; Erkortal, B.; Chakravadhanula, V.S.K.; Kienle, L.; Grundmeier, G.; Garbe-Schoenberg, D.; et al. Tuning of the ion release properties of silver nanoparticles buried under a hydrophobic polymer barrier. *J. Nanoparticle Res.* **2012**, *14*, 928. [[CrossRef](#)]
22. Baran, A.; Baran, M.F.; Keskin, C.; Kandemir, S.I.; Valiyeva, M.; Mehraliyeva, S.; Khalilov, R.; Eftekhari, A. Ecofriendly/Rapid Synthesis of Silver Nanoparticles Using Extract of Waste Parts of Artichoke (*Cynara scolymus* L.) and Evaluation of their Cytotoxic and Antibacterial Activities. *J. Nanomater.* **2021**, *2021*, 2270472. [[CrossRef](#)]
23. Duran, N.; Nakazato, G.; Seabra, A.B. Antimicrobial activity of biogenic silver nanoparticles, and silver chloride nanoparticles: An overview and comments. *Appl. Microbiol. Biotechnol.* **2016**, *100*, 6555–6570. [[CrossRef](#)] [[PubMed](#)]

24. Li, H.; Wang, Y.; Wang, S.; Wang, B.; Wang, X.; Mi, Z.; Fu, J.; Zhang, Z.; Yan, W. Enhancing the Stability of the Resin–Dentin Bonding Interface with Ag<sup>+</sup>- and Zn<sup>2+</sup>-Exchanged Zeolite A. *ACS Biomater. Sci. Eng.* **2022**, *8*, 1717–1725. [[CrossRef](#)] [[PubMed](#)]
25. Giraldo, L.F.; Camilo, P.; Kyu, T. Incorporation of silver in montmorillonite-type phyllosilicates as potential antibacterial material. *Curr. Opin. Chem. Eng.* **2016**, *11*, 7–13. [[CrossRef](#)]
26. Binay, M.I.; Kirdeciler, S.K.; Akata, B. Development of antibacterial powder coatings using single and binary ion-exchanged zeolite A prepared from local kaolin. *Appl. Clay Sci.* **2019**, *182*, 245–251. [[CrossRef](#)]
27. Roy, A.; Butola, B.S.; Joshi, M. Synthesis, characterization and antibacterial properties of novel nano-silver loaded acid activated montmorillonite. *Appl. Clay Sci.* **2017**, *146*, 278–285. [[CrossRef](#)]
28. Shameli, K.; Bin Ahmad, M.; Zargar, M.; Yunus, W.M.Z.W.; Ibrahim, N.A.; Shabanzadeh, P.; Moghaddam, M.G. Synthesis and characterization of silver/montmorillonite/chitosan bionanocomposites by chemical reduction method and their antibacterial activity. *Int. J. Nanomed.* **2011**, *6*, 271–284. [[CrossRef](#)] [[PubMed](#)]
29. Shameli, K.; Ahmad, M.B.; Zargar, M.; Yunus, W.M.Z.W.; Rustaiyan, A.; Ibrahim, N.A. Synthesis of silver nanoparticles in montmorillonite and their antibacterial behavior. *Int. J. Nanomed.* **2011**, *6*, 581–590. [[CrossRef](#)] [[PubMed](#)]

**Disclaimer/Publisher’s Note:** The statements, opinions and data contained in all publications are solely those of the individual author(s) and contributor(s) and not of MDPI and/or the editor(s). MDPI and/or the editor(s) disclaim responsibility for any injury to people or property resulting from any ideas, methods, instructions or products referred to in the content.